

# The Auroral Ionosphere: Comparison of a Time-Dependent Model With Composition Measurements

J.-C. GERARD<sup>1</sup> AND D. W. RUSCH<sup>2</sup>

*Space Physics Research Laboratory, Department of Atmospheric and Oceanic Science  
University of Michigan, Ann Arbor, Michigan 48109*

A time-dependent model of the auroral ionosphere including the odd nitrogen species, NO, N(<sup>2</sup>D), and N(<sup>4</sup>S), is used for comparison with data from a coordinated rocket-satellite measurement of an auroral event. The chemical scheme and the adopted rate coefficients have been shown to be compatible with daytime mid-latitude ionospheric chemistry. The electron flux and neutral atmospheric parameters measured on the satellite are used to compute the appropriate ionization and dissociation rates. The calculated NO<sup>+</sup>, O<sub>2</sub><sup>+</sup>, O<sup>+</sup>, Ne, and NO densities agree well with the rocket measurements. The calculated N<sub>2</sub><sup>+</sup> densities are larger than the measured densities by a factor of 3 at most altitudes. The calculations show that the nitric oxide content of the aurora (~1.2 × 10<sup>8</sup> NO molecules/cm<sup>3</sup> at 105 km) is below the saturation value.

## INTRODUCTION

During the last decade, several measurements of the composition of the auroral ionosphere have been made using rocket-borne mass spectrometers. They have been recently reviewed by *Swider and Narcisi* [1977] and generally show that the amount of NO<sup>+</sup> ions in the *E* region is enhanced by a variable factor with respect to the daytime mid-latitude conditions. The high NO<sup>+</sup>/O<sub>2</sub><sup>+</sup> ratio measurement by *Donahue et al.* [1970] led them to speculate that charge exchange of O<sub>2</sub><sup>+</sup> ions with enhanced amounts of nitric oxide or atomic nitrogen may be responsible for the increase of the NO<sup>+</sup> density. Subsequently, measurements of this ratio during steady state auroral conditions have been used to infer the amount of nitric oxide present in the auroral *E* region [*Swider and Narcisi*, 1974; *Narcisi and Swider*, 1976; *Swider and Narcisi*, 1977]. Satellite measurements of the intensity of the nitric oxide  $\gamma$  band resonance scattering in twilight have also indicated that the amount of NO is higher and more variable at high latitudes than at mid-latitude [*Rusch and Barth*, 1975] and that the NO density responds to the auroral activity during severe magnetic storms [*Gerard and Barth*, 1977].

Various models have been developed to examine how the odd nitrogen densities are affected by particle precipitation in the *E* region [*Jones and Rees*, 1973; *Vallance-Jones*, 1975; *Hyman et al.*, 1976; *Gerard and Barth*, 1977; *Roble and Rees*, 1977]. They show that significant buildup of nitric oxide may be obtained provided the atomic nitrogen atoms resulting from the increased ionization and dissociation of N<sub>2</sub> are mainly produced in the metastable N(<sup>2</sup>D) state. However, the results of these calculations could not be tested quantitatively against actual observations, since simultaneous determination of the precipitated electron spectrum as well as the neutral and ionic composition was missing. Such a requirement on the fraction of N(<sup>2</sup>D) produced is in agreement with the analysis of the daytime N(<sup>2</sup>D) and NO densities [*Frederick and Rusch*, 1977; *Cravens et al.*, 1979].

In this study we take advantage of a successfully coordinated measurement of the electron spectrum, electron temper-

ature, and neutral composition by experiments on board the Atmosphere Explorer C satellite and simultaneous rocket measurements of ion composition and airglow reported by *Rees et al.* [1977] and *Sharp et al.* [1979]. Our aim is to determine whether the observed ionosphere and the nitric oxide may be modeled adequately by a time-dependent calculation using the daytime chemistry and being constrained by a large number of observed quantities. The nitric oxide density was inferred from a measurement of the NO<sub>2</sub> continuum on the same flight [*Sharp*, 1978].

## MODEL

The launch conditions of the rocket whose data will be analyzed here have been described in detail by *Rees et al.* [1977] and will not be repeated here. Suffice it to say that the rocket launch was coordinated with a pass of the AE-C satellite over Fort Churchill at an altitude of 490 km. During the period the intensity of the N<sub>2</sub><sup>+</sup> first negative band at 3914 Å was 4 kR, but a brighter display had been observed prior to the launch. The aurora remained relatively time invariant during the flight as could be judged from the ground-based and rocket measurements of the 3914-Å intensity. The energy spectrum of the precipitated electrons was measured by the low-energy electron detector (LEE) [*Hoffman et al.*, 1973] on the AE-C satellite. The neutral atmospheric composition was measured by the open source mass spectrometer [*Nier et al.*, 1973] on the satellite between 470 and 200 km and showed only small latitudinal gradients as determined by comparisons of downleg to upleg data.

At lower altitudes the densities are obtained by extrapolating downward assuming diffusive equilibrium. The density profiles obtained agree well with those inferred from the photometric rocket data down to near the base of the aurora [*Sharp et al.*, 1979] and are listed in Table 1. This atmospheric composition is remarkable in that it shows an unusually large O<sub>2</sub>/O ratio at all altitudes. For example, it is 3 times richer in O<sub>2</sub> and 3 times poorer in O at 200 km than the MSIS model [*Hedin et al.*, 1977] corresponding to the observed N<sub>2</sub> profile. There is no indication from either the rocket or the satellite data of any unusual structure in the neutral density profiles. Surely, the unusually large O<sub>2</sub>/O ratio indicates that the atmosphere is adjusting to auroral heating and induced vertical winds. It is not the purpose of this paper to quantitatively examine the neutral density profiles. Suffice it to say that vertical winds would tend to produce an O<sub>2</sub>/O ratio larger

<sup>1</sup> Also with Institut D'Astrophysique, Université de Liège, Coite-Ougrée, Belgium.

<sup>2</sup> Now at Laboratory for Atmospheric and Space Physics, University of Colorado, Boulder, Colorado 80309.

TABLE 1. Neutral Atmosphere, 4278 Emission, and Ion Production Rates

Z, km	$T_n$ , °K	$N_2$ , $\text{cm}^{-3}$	O, $\text{cm}^{-3}$	$O_2$ , $\text{cm}^{-3}$	$I_{4278}$ , photons $\text{cm}^{-2} \text{s}^{-1}$	$I_{N_2^+}$ , $\text{cm}^{-2} \text{s}^{-1}$	$I_{O^+}$ , $\text{cm}^{-2} \text{s}^{-1}$	$I_{O_2^+}$ , $\text{cm}^{-2} \text{s}^{-1}$
90	187	4.9(13)	7.9(10)	1.3(13)	23.0	8.8(3)	9.2(1)	1.8(2)
100	195	8.7(12)	1.4(11)	1.9(12)	914	3.5(4)	4.0(3)	7.3(3)
102.5	204	5.6(12)	1.2(11)	1.1(12)	952	3.6(4)	4.2(3)	7.3(3)
105	213	3.6(12)	1.1(11)	7.0(11)	881	3.3(4)	3.9(3)	6.4(3)
110	250	1.6(12)	7.4(10)	2.7(11)	58.1	2.2(3)	2.7(3)	3.8(3)
130	529	1.3(11)	1.5(10)	1.8(10)	95.2	3.6(3)	5.4(2)	4.9(2)
150	716	3.6(10)	5.5(9)	4.3(9)	31.1	1.2(3)	2.0(2)	1.4(2)
170	826	1.4(10)	2.5(9)	1.5(9)	13.3	5.0(2)	9.4(1)	5.3(1)
190	890	6.3(9)	1.4(9)	6.0(8)	6.4	2.4(2)	5.1(1)	2.3(1)
210	927	3.0(9)	8.3(8)	2.6(8)	3.3	1.3(2)	3.1(1)	1.1(1)
230	949	1.5(9)	6.6(8)	1.2(8)	1.9	7.1(1)	2.1(1)	5.5(0)

Read 4.9(13) as  $4.9 \times 10^{13}$ .

than normal and that the measurements are consistent with this expectation.

The ionization rate profile is calculated by using a method developed by Lazarev [1967] for the case of a monodirectional monoenergetic beam. This formula gives an analytical expression for the total ionization rate as a function of the penetration depth and depends on the energy of the primary electrons and the local mass density [Gerard, 1970]. To illustrate its validity, Figure 1 shows the altitude distribution of the total ionization rate for a unit flux of incident electrons of three different energies. It is compared with the profile calculated by Berger *et al.* [1970] using a Monte-Carlo calculation for the degradation of the electrons. In this comparison, the same neutral composition is used, the Jacchia [1971] model for an exospheric temperature of 1050°K. The agreement between the two methods is very good, both in shape and in magnitude for 20-keV electrons; it is within 30% for a 2-keV precipitation. Consequently, we feel confident that this method yields reliable auroral ionization profiles. To model the particular event we are analyzing, the electron spectrum measured by

LEE at universal time 15368 s is used as input, together with the neutral atmospheric composition listed in Table 1. The ionization rate is integrated over the energy spectrum, and an isotropic pitch angle distribution from 0° to 80° is assumed, in agreement with the pitch angle distribution measured by the detectors. Because of the shape of the measured electron energy spectrum, there is reason to believe that high-energy electrons are present beyond the instrument threshold of 25 keV. We have therefore performed two calculations: one extrapolating the LEE energy spectrum to higher energies than was done by Rees *et al.* [1977], and the other assuming no flux above 25 keV. The volume emission rate of the  $\lambda 3914$ -Å band of the  $N_2^+$  first negative system,  $\eta(3914)$ , is calculated from the total ionization rate  $q$  by using

$$\eta(3914) = q \frac{0.88[N_2]}{0.88[N_2] + 0.5[O] + [O_2]} \frac{1}{14.7}$$

[Vallance-Jones, 1975]. The resulting distribution of the vertical column emission rate is shown in Figure 2 and compared with the rocket photometer measurement. The two curves agree very well at high altitude, but the calculated intensity progressively exceeds the measurements as altitude decreases. At 90 km the ratio of the calculated to the measured intensity is approximately 2 for the extrapolated flux and 1.4 for the case when no extrapolation was made. A similar problem was encountered by Rees *et al.* [1977], whose calculated 3914-Å intensity is approximately twice the observed intensity at all altitudes. No satisfactory interpretation can be given to the discrepancy except that the correlation between the satellite and the rocket was only realized when the latter was at 217 km. The electron spectrum or pitch angle distribution may have been different when the rocket entered the auroral ionization peak. Since a better agreement with the measured 3914-Å profile was obtained from the actual electron measurement, it will be used in the following calculation. The calculated ionization rates for  $N_2$ ,  $O_2$ , and O are shown in Table 1.

The production rates of individual ions are obtained from the total ion production rate  $q$  following the method described by Vallance-Jones [1975]. The relative production of  $O^+$  ions in the three lower levels  $^4S$ ,  $^2D$ , and  $^2P$  is 0.48, 0.32, and 0.20 of the total  $O^+$  production, respectively.

The ion and odd nitrogen densities are calculated by using a time-dependent model described by Rusch *et al.* [1977a] and Cravens *et al.* [1979]. The program uses a general second-order differential equation solver developed at the National Center for Atmospheric Research by Hastings and Roble [1977]. The continuity equations are solved for  $N_2^+$ ,  $NO^+$ ,  $O_2^+$ ,  $N^+$ ,  $O^+$

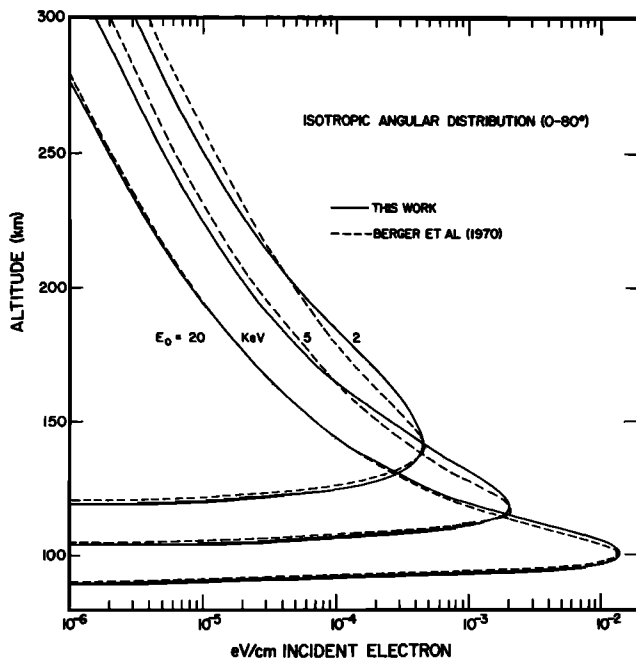


Fig. 1. Comparison of the total ionization rate versus altitude for a unit flux of incident electrons for 2, 5, and 20 keV between this work and Berger *et al.* [1970].

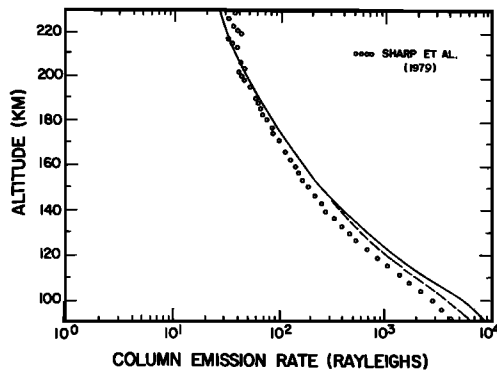


Fig. 2. The vertical column emission rate of 3914-Å emission versus altitude for this work compared to the measurement of Sharp *et al.* [1979].

( $^4S$ ),  $O^+(^2D)$ ,  $O^+(^2P)$ ,  $N(^2D)$ ,  $N(^2P)$ ,  $N(^4S)$ , and  $NO$  with the chemical reactions listed in Table 2. The  $NO$  and  $N(^4S)$  calculations include molecular and eddy diffusion and appropriate flux conditions at the lower (50 km) and upper (250 km) boundaries. Most of the reaction rates and their temperature dependence used in the calculations have been measured in the laboratory, and their values have been confirmed by the analysis of the *AE* measurements of the thermospheric ion composition [Torr and Torr, 1978]. However, a few branching ratios and quenching rates have not been experimentally determined, and a choice must be made guided by our knowledge of the

odd nitrogen daytime chemistry. The reaction of  $N_2^+$  with  $O$  (reaction (R7)) is assumed to produce only  $N(^2D)$  atoms, and the dissociation of  $N_2$  by fast electron impact yields 75% of  $N(^2D)$  and 25% of  $N(^4S)$  in the model. The values are in agreement with the [N I] 5200-Å airglow analysis by Frederick and Rusch [1977] and give satisfactory agreement with the nitric oxide densities observed in the mid-latitude lower thermosphere [Cravens *et al.*, 1979].

## RESULTS

As was mentioned earlier, the enhanced dissociation and ionization of  $N_2$  due to the particle precipitation produced an increase of the nitric oxide sources in the *E* region. Consequently, in an atmosphere subject to constant particle flux, the nitric oxide density increases with time until a saturation is reached.

In Figure 3 the results of three time-dependent calculations are shown. Case 1 (solid lines) shows the  $NO$  buildup and development of the  $NO^+/O_2^+$  ratio using the ionization rate profile described in the text at all times. Case 2 (dashed lines) uses a two-step ionization rate such that the initial ionization rate is 10 times the measured one for the first  $2 \times 10^9$  s of computation. The ionization rate is then decreased to the measured value with a 10-s exponential decay and then held constant. Case 3 (dotted lines) represents a calculation similar to case 2 except that the time is for the larger flux in  $3 \times 10^9$  s. Starting from  $2 \times 10^7$   $cm^{-3}$ , the  $NO$  density in case 1 varies little during the first  $10^9$  seconds but increases to  $2 \times 10^9$   $cm^{-3}$

TABLE 2. Reactions and Reaction Rates

No.	Reaction	Reaction Rate*	Source
(R1)	$O + e \rightarrow O^+(^4S, ^2D, ^2P) + 2e$	see text†	$f$ 's from Torr and Torr [1978]
(R2)	$O_2 + e \rightarrow O_2^+ + 2e$	see text	
(R3)	$O_2 + e \rightarrow O + O^+(^4S, ^2D, ^2P) + 2e$	see text†	
(R4)	$N_2 + e \rightarrow N_2^+ + 2e$	see text	
(R5)	$N_2 + e \rightarrow N(^4S) + N(^2D, ^2P) + e$	see text	
(R6)	$N_2 + e \rightarrow N(^4S, ^2D, ^2P) + N^+ + 2e$	see text	
(R7)	$N_2^+ + O \rightarrow NO^+ + N(^2D)$	$1.4 \times 10^{-10}(T/300)^{-0.44}$	McFarland <i>et al.</i> [1974]
(R8)	$N_2^+ + O_2 \rightarrow O_2^+ + N_2$	$5 \times 10^{-11}(T/300)^{-0.8}$	Lindinger <i>et al.</i> [1974]
(R9)	$N_2^+ + e \rightarrow N(^4S) + N(^2D)$	$1.8 \times 10^{-7}(T/300)^{-0.89}$	Mehr and Biondi [1969]
(R10)	$O^+ + N_2 \rightarrow NO^+ + N(^4S)$	$5 \times 10^{-18}$	Lindinger <i>et al.</i> [1974]
(R11)	$O^+ + O_2 \rightarrow O_2^+ + O$	$2 \times 10^{-11}(T_e/300)^{-0.4}$	McFarland <i>et al.</i> [1974]
(R12)	$O_2^+ + NO \rightarrow NO^+ + O_2$	$4.4 \times 10^{-10}$	Lindinger <i>et al.</i> [1974]
(R13)	$O_2^+ + N(^2D) \rightarrow NO^+ + O$	$1.8 \times 10^{-10}$	Goldan <i>et al.</i> [1966]
(R14)	$O_2^+ + e \rightarrow O + O$	$1 \times 10^{-6}T_e^{-0.7}$	Torr <i>et al.</i> [1976a]
(R15)	$N^+ + O_2 \rightarrow NO^+ + O$	$2.75 \times 10^{-10}$	McFarland <i>et al.</i> [1973]
(R16)	$NO^+ + e \rightarrow N(^4S, ^2D) + O$	$4.2 \times 10^{-7}(T_e/300)^{-0.88}$	Walls and Dunn [1974]
(R17)	$N(^4S) + O_2 \rightarrow NO + O$	$2.4 \times 10^{-11} \exp(-3975/T_n)$	Wilson [1967]
(R18)	$N(^2D) + O_2 \rightarrow NO + O$	$6 \times 10^{-12}$	Lin and Kaufman [1971]
(R19)	$N(^2D) + e \rightarrow N(^4S) + e$	$6 \times 10^{-10}(T_e/300)^{0.8}$	Frederick and Rusch [1977]
(R20)	$N(^2D) + O \rightarrow N(^4S) + O$	$5 \times 10^{-13}$	Frederick and Rusch [1977]
(R21)	$N(^4S) + NO \rightarrow N_2 + O$	$2.1 \times 10^{-11}$	Phillips and Schiff [1962]
(R22)	$N(^2D) \rightarrow N(^4S) + h\nu_{6300}$	$A_{2D} = 1.07 \times 10^{-6} s^{-1}$	Garstang [1956]
(R23)	$O^+(^2D) + N_2 \rightarrow N_2^+ + O$	$1 \times 10^{-9}$	Rutherford and Vroom [1971]
(R24)	$N(^2P) + O \rightarrow N(^2D) + O$	$1 \times 10^{-11}$	Young and Dunn [1975]
(R25)	$N(^2P) + e \rightarrow N(^2D) + e$	$6 \times 10^{-10}(T_e/300)^{0.5}$	Assumed
(R26)	$N(^2P) \rightarrow N(^2D) + h\nu$	$A = 0.079 s^{-1}$	Garstang [1956]
(R27)	$N(^2P) \rightarrow N(^4S) + h\nu$	$A = 0.005 s^{-1}$	Garstang [1956]
(R28)	$O^+(^2P) + O \rightarrow O^+(^2D) + O$	$5.2 \times 10^{-11}$	Rusch <i>et al.</i> [1977]
(R29)	$O^+(^2P) + e \rightarrow O^+(^2D) + e$	$1.89 \times 10^{-7}(T_e/300)^{-0.5}$	Henry <i>et al.</i> [1970]
(R30)	$O^+(^2P) \rightarrow O^+(^2D) + h\nu$	$A = 0.17 s^{-1}$	Seaton and Osterbrook [1957]
(R31)	$O^+(^2P) \rightarrow O^+(^4S) + h\nu$	$A = 0.048 s^{-1}$	Seaton and Osterbrook [1957]
(R32)	$O^+(^2P) + N_2 \rightarrow N_2^+ + O$	$4.8 \times 10^{-10}$	Rusch <i>et al.</i> [1977]
(R33)	$N(^2D) + NO \rightarrow N_2 + O$	$7 \times 10^{-11}$	Black <i>et al.</i> [1969]
(R34)	$N(^2P) + O_2 \rightarrow NO + O$	$2.6 \times 10^{-12}$	Husain <i>et al.</i> [1974]

\*Rates are in units of  $cm^3 s^{-1}$  unless otherwise noted.

† $f(^4S) = 0.484$ ,  $f(^2D) = 0.323$ ,  $f(^2P) = 0.194$ .

‡ $f(^4S)$ ,  $f(^2D)$ ,  $f(^2P)$ , same as for (R1).

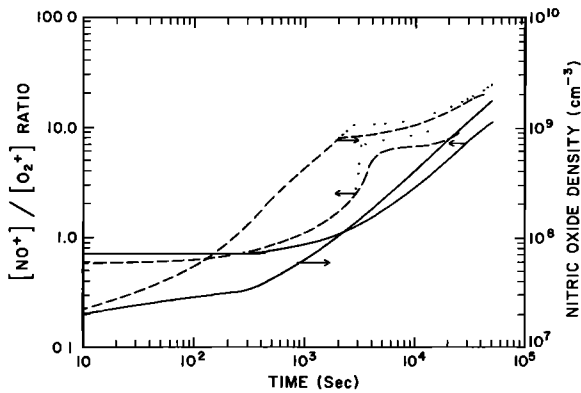


Fig. 3. Nitric oxide density and  $\text{NO}^+/\text{O}_2^+$  ratio versus time. The solid lines correspond to the ionizing flux measured by LEE. The dashed lines correspond to a flux of 10 times the measured one for  $2 \times 10^3$  s and then a decay to the measured flux. The dotted lines correspond to a flux of 10 times the measured one for  $3 \times 10^3$  s and then a decay to the measured flux.

after  $5 \times 10^4$  s. As a consequence,  $\text{O}_2^+$  ions are progressively converted into  $\text{NO}^+$  through reaction (R12), and the  $\text{NO}^+/\text{O}_2^+$  ratio increases from 0.7 to 12. The ratio of  $\text{NO}^+/\text{O}_2^+$  observed at 105 km by the rocket mass spectrometer is observed in the model after about  $3 \times 10^4$  s.

We recognize that the assumption of a constant precipitation during a time period of several times  $10^4$  seconds is unrealistic. However, a more intense electron flux could produce the same result in a shorter time, since the density of NO depends only on the total integrated energy flux and the fraction of  $\text{N}(^2D)$  and  $\text{N}(^4S)$  atoms produced by reactions (R5), (R6), (R7), and (R16). In fact, a strong breakup period preceded this aurora and was probably able to generate in a few minutes most of the NO present in this aurora. Cases 2 and 3 are attempts to simulate this situation. The energy deposition in the atmosphere above Fort Churchill was nearly constant for about 1000 s before the rocket launch and remained constant during the upleg portion of the flight. Previous to this, the large breakup deposited an average energy of nearly 10 times the energy at launch for several thousand seconds (W. E. Sharp, private communication, 1978).

In case 2 the measured  $\text{NO}^+/\text{O}_2^+$  ratio is achieved after  $1.6 \times 10^4$  s and in case 3 after  $3.1 \times 10^3$  s. In case 3 most of the nitric oxide owes its existence to the larger flux. In each case, however, the electron density is present in response to the low flux. The time constant for the ionosphere to come into equilibrium with the incident flux is about 500 s at 190 km and about 60 s at 110 km. Thus all three cases produce essentially the same ion density profiles at the time when the  $\text{NO}^+/\text{O}_2^+$  ratio is equal to the measurement, and the observed electron density is consistent with the measured ionization rate. In case 3 the observations produce the  $\text{NO}^+/\text{O}_2^+$  ratio in less than 1 hour. We realize that minor constituents are subject to transport by vertical and horizontal winds and will be transported out of the vicinity of their creation, possibly with very short time constants. A horizontal wind of 30 m/s would remove the nitric oxide generated in a  $1^\circ$  wide auroral arc in 1 hour. While we do not claim to have exactly represented the time history of this particular aurora, we do, however, feel that the results are consistent with the scenario adopted and that (1) nitric oxide densities of several times  $10^9/\text{cm}^3$  can be generated in auroral arcs and the agreement between the calculated NO density at 110 km (see Figure 6) indicates that the time constant for this buildup was less than the time constant for its horizontal or

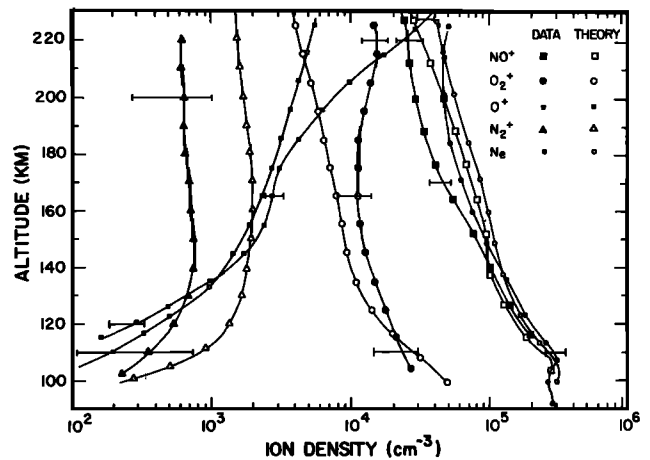


Fig. 4. Comparison between the calculated and observed ionospheric densities at  $t = 5 \times 10^4$  s using the  $\text{NO}^+$  dissociative recombination rate of Walls and Dunn [1974].

vertical dispersion and (2) the agreement between the measured and calculated ion densities (see Figure 5) shows that the electron density resulted from the measured ionization rate. We illustrate the calculated ion composition at that time in Figures 4 and 5. It may be seen that a good agreement with the observations is obtained for most ions. The detailed comparison will be discussed in the next section.

The altitude distributions of  $\text{N}(^2D)$ ,  $\text{N}(^4S)$ , and NO are shown in Figure 6 for the time when the  $\text{NO}^+/\text{O}_2^+$  ratio was in agreement with the measurement. In this case the  $\text{N}(^2D)$  and  $\text{N}(^4S)$  densities are nearly equal, in contrast to the daytime situation, where  $[\text{N}(^4S)] \sim 20[\text{N}(^2D)]$  at 180 km. The NO densities are enhanced with respect to mid-latitude conditions by more than an order of magnitude. The NO density at 110 km derived by Sharp [1978] from the intensity of the  $\text{NO}_2$  continuum measured on the same flight is also indicated in Figure 6. The agreement between the two methods strongly supports the validity of the deduced NO density.

#### DISCUSSION AND CONCLUSIONS

We have used a time-dependent model of the auroral ionosphere which includes a detailed calculation of the odd nitrogen chemistry to compare it with a comprehensive set of coordinated rocket and satellite measurements. The absolute densities of  $\text{NO}^+$ ,  $\text{O}_2^+$ ,  $\text{O}^+$ , and  $\text{N}_2^+$  are compared at the time

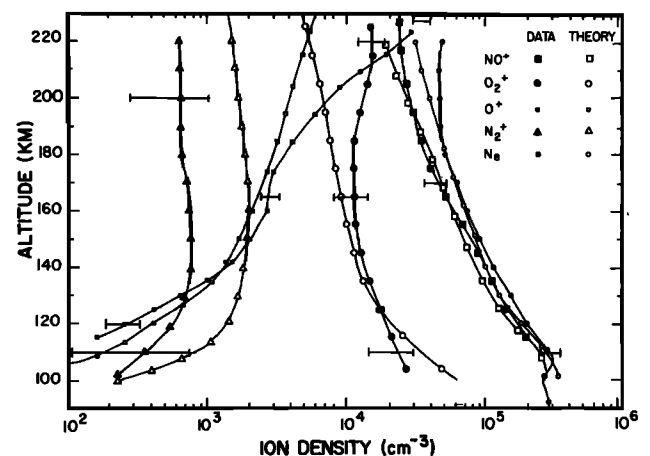


Fig. 5. Same as Figure 4 except that the Huang et al. [1975] rate is adopted for the  $\text{NO}^+$  recombination rate.

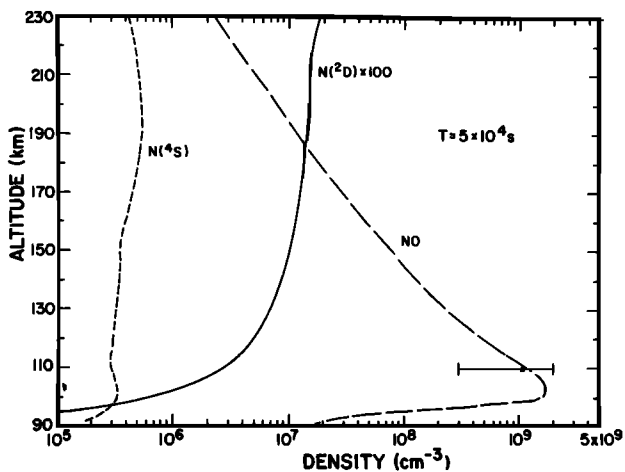


Fig. 6. The calculated altitude distributions of NO,  $N(^2D)$ , and  $N(^4S)$ . The measurement of Sharp [1978] is included for comparison.

when the model predicts the  $\text{NO}^+/\text{O}_2^+$  ratio. The comparison between the calculated and measured  $\text{NO}^+$ ,  $\text{O}_2^+$ , and  $\text{O}^+$  densities is excellent, especially at low altitudes, and the calculated NO density agrees well with that determined from the measured  $\text{NO}_2$  continuum emission [Sharp, 1978]. Note that the NO density at the time of the measurement is well below its saturation value.

The calculated and measured  $\text{O}^+$  densities agree well below 190 km. The major source of  $\text{O}^+$  at low altitudes ( $Z < 150$  km) is dissociative ionization of  $\text{O}_2$ , and we have assumed that the  $\text{O}^+$  ions produced by this reaction are found in metastable states in the same proportion as direct impact ionization of O. Thus less than 50% of the  $\text{O}^+$  ions are formed in the ground state. Metastable  $\text{O}^+$  ions are lost far more rapidly than ground state  $\text{O}^+$  (see Table 2), and this accounts in part for the excellent agreement.

Two difficulties remain: The measured ion densities diverge from the theory at high altitudes, and the calculated  $\text{N}_2^+$  densities are nearly a factor of 3 higher at most altitudes.

The detailed comparison between the calculated and measured 3914-Å emission is instructive in the first case. In the work of Rees *et al.* [1977] the measured 3914-Å emission changes slope above 180 km and indicates an increased ionization rate. This would account for the increased ion density at high altitudes.

The  $\text{N}_2^+$  problem is more difficult to understand. In each of the models the calculated  $\text{N}_2^+$  is a factor of 3 higher than the measurements at most altitudes and approaches the measured  $\text{N}_2^+$  at low altitudes.

The chemistry of  $\text{N}_2^+$  is straightforward, the loss processes being charge exchange with  $\text{O}_2$  at low altitude and the ion atom interchange reaction with O at high altitude. Also it appears that the higher recombination rate for  $\text{NO}^+$  of Huang *et al.* [1975] better describes the  $\text{NO}^+$  density distribution. This recombination rate is not consistent with the mid-latitude studies of Torr *et al.* [1976b] and may be deceiving inasmuch as the  $\text{NO}^+$  is produced mainly by  $\text{N}_2^+ + \text{O}$  at high altitudes. The  $\text{NO}^+$  density may be too large in Figure 4 as a direct result of the high  $\text{N}_2^+$ . The Huang *et al.* [1975] rate is probably correct for vibrationally excited  $\text{NO}^+$  and if applicable to the aurora would imply that  $\text{NO}^+$  is vibrationally excited. But the sources of  $\text{NO}^+$  ions in the aurora are the same as those in the dayglow, and so we should not expect  $\text{NO}^+$  to be found in an enhanced vibrational state. Also, in recent calculations, Swider

and Narcisi [1977], Narcisi and Swider [1976], and Swider and Narcisi [1974] appear to have the same problem with the calculated  $\text{N}_2^+$  densities when the neutral atmosphere adopted is one of relatively low atomic oxygen concentration.

We stress further need for broad-based measurements of auroral conditions which can serve as constraints on model calculations.

**Acknowledgments.** The authors thank W. E. Sharp for making his data available and for his helpful discussions. This work was supported by the National Aeronautics and Space Administration under grants NSG 5171, NAS5-23006, and NGR23-005-360. One of the authors (J.-C.G.) is supported by the Belgian Foundation for Scientific Research (FNRS). We thank the National Center for Atmospheric Research for computer time. The National Center for Atmospheric Research is sponsored by the National Science Foundation.

The Editor thanks R. G. Roble and M. H. Rees for their assistance in evaluating this paper.

## REFERENCES

- Berger, M. J., S. M. Saltzer, and K. Maeda, Energy deposition by auroral electrons in the atmosphere, *J. Atmos. Terr. Phys.*, **32**, 1015, 1970.
- Black, G., T. G. Stanger, G. A. St. John, and R. A. Young, Vacuum ultraviolet photolysis of  $\text{N}_2\text{O}$ , 4, Deactivation, *J. Chem. Phys.*, **51**, 116, 1969.
- Cravens, T. E., J.-C. Gerard, A. I. Stewart, and D. W. Rusch, The latitudinal gradient of nitric oxide in the lower thermosphere, submitted to *J. Geophys. Res.*, 1979.
- Donahue, T. M., E. C. Zipf, and T. D. Parkinson, Ion composition and ion chemistry in an aurora, *Planet. Space Sci.*, **18**, 171, 1970.
- Frederick, J. E., and D. W. Rusch, On the chemistry of metastable atomic nitrogen in the F region deduced from simultaneous satellite measurements of the 5200-Å airglow and atmospheric composition, *J. Geophys. Res.*, **82**, 3509, 1977.
- Garstang, R. A., Transition probabilities of auroral lines, in *The Airglow and Aurorae*, edited by E. B. Armstrong, p. 324, Pergamon, New York, 1956.
- Gerard, J.-C., Metastable oxygen ions distribution in aurora, *Ann. Geophys.*, **26**, 777, 1970.
- Gerard, J.-C., and C. A. Barth, High-latitude nitric oxide in the lower thermosphere, *J. Geophys. Res.*, **82**, 674, 1977.
- Goldan, P. D., A. L. Schmeltekopf, F. C. Fehsenfeld, H. I. Schiff, and E. E. Ferguson, Thermal energy ion-neutral reaction rates, 2, Some reactions of ionospheric interest, *J. Chem. Phys.*, **44**, 4095, 1966.
- Hastings, J. T., and R. G. Roble, An automatic technique for solving coupled vector systems of nonlinear parabolic partial differential equations in one space dimension, *Planet. Space Sci.*, **25**, 209-215, 1977.
- Hedin, A. E., C. A. Reber, G. P. Newton, N. W. Spencer, H. C. Brinton, H. G. Mayr, and W. E. Potter, A global thermospheric model based on mass spectrometer and incoherent scatter data MSIS, 2, Composition, *J. Geophys. Res.*, **82**, 2148, 1977.
- Henry, R. J. W., Photo-ionization cross sections for atoms and ions of carbon, nitrogen, oxygen, and neon, *Astrophys. J.*, **161**, 1153, 1970.
- Hoffman, P. A., J. L. Burch, R. W. Janetzke, J. F. McChesner, S. H. Way, and D. S. Evans, Low-energy electron experiment for Atmosphere Explorer C and D, *Radio Sci.*, **8**, 393, 1973.
- Huang, C. M., M. A. Biondi, and R. Johnson, Variation of electron- $\text{NO}^+$  ion recombination coefficient with electron temperature, *Phys. Rev. A*, **11**, 901, 1975.
- Husain, D., S. K. Mitra, and A. N. Young, Kinetic study of electronically excited atoms  $\text{N}(^2D_j, ^2P_j)$  by attenuation of atomic resonance radiation in the vacuum ultraviolet, *J. Chem. Soc. Faraday Trans. 2*, **70**, 1721, 1974.
- Hyman, E., D. J. Strickland, P. S. Julienne, and D. F. Strobel, Auroral NO concentrations, *J. Geophys. Res.*, **81**, 4765, 1976.
- Jacchia, L. G., Revised static models of thermosphere and exosphere with empirical temperature profiles, Spec. Rep. 332, Smithsonian Astrophys. Observ., Cambridge, Mass., May 1971.
- Jones, R. A., and M. H. Rees, Time-dependent studies of the aurora, 1, Ion density and composition, *Planet. Space Sci.*, **21**, 537, 1973.
- Lazarev, V. I., Absorption of the energy of an electron beam in the upper atmosphere, *Geomagn. Aeron.*, **7**, 219, 1967.
- Lin, C.-L., and F. Kaufman, Reactions of metastable nitrogen atoms, *J. Chem. Phys.*, **53**, 3760, 1971.

- Lindinger, W., F. C. Fehsenfeld, A. L. Schmeltekopf, and E. E. Ferguson, Temperature dependence of some ionospheric ion-neutral reactions from 300° to 900°K, *J. Geophys. Res.*, **79**, 4753, 1974.
- McFarland, M., D. L. Albritton, F. C. Fehsenfeld, E. E. Ferguson, and A. L. Schmeltekopf, A flow-drift technique for ion mobility and ion-molecule rate constant measurements, *J. Chem. Phys.*, **59**, 6620, 1973.
- McFarland, M., D. L. Albritton, F. C. Fehsenfeld, E. E. Ferguson, and A. L. Schmeltekopf, Energy dependence and branching ratio of the  $N_2^+ + O$  reaction, *J. Geophys. Res.*, **79**, 2925, 1974.
- Mehr, F. J., and M. A. Biondi, Electron temperature dependence of recombination of  $O_2^+$  and  $N_2^+$  ions with electrons, *Phys. Rev.*, **181**, 264, 1969.
- Narcisi, R. S., and W. Swider, Ionic structure near an auroral arc, *J. Geophys. Res.*, **81**, 4770, 1976.
- Nier, A. O., W. E. Potter, D. R. Hickman, and K. Mauersberger, The open source neutral mass spectrometer on Atmosphere Explorer C, D, and E, *Radio Sci.*, **8**, 271, 1973.
- Phillips, L. F., and H. I. Schiff, Mass spectrometer studies of atom reactions, 1, Reactions in the atomic nitrogen-ozone system, *J. Chem. Phys.*, **36**, 1509, 1962.
- Rees, M. H., A. I. Stewart, W. E. Sharp, P. B. Hays, R. A. Hoffman, L. H. Brace, J. P. Doering, and W. K. Peterson, Coordinated rocket and satellite measurements of an auroral event, 1, Satellite observations and analysis, *J. Geophys. Res.*, **82**, 2250, 1977.
- Roble, R. G., and M. H. Rees, Time-dependent studies of the aurora: Effects of particle precipitation on the dynamic morphology of ionospheric and atmospheric properties, *Planet. Space Sci.*, **25**, 991, 1977.
- Rusch, D. W., and C. A. Barth, Satellite measurements of nitric oxide in the polar region, *J. Geophys. Res.*, **80**, 3719, 1975.
- Rusch, D. W., T. E. Cravens, G. R. Carignan, A. I. Stewart, and J.-C. Gerard, A theoretical model of odd nitrogen in the earth's thermosphere and mesosphere (abstract), *Eos Trans. AGU*, **58**, 1198, 1977a.
- Rusch, D. W., D. G. Torr, P. B. Hays, and J. C. G. Walker, The O II (7319-30 Å) dayglow, *J. Geophys. Res.*, **82**, 719, 1977b.
- Rutherford, J. A., and D. G. Vroom, Effect of metastable  $O^+(^2D)$  on reactions of  $O^+$  with nitrogen molecules, *J. Chem. Phys.*, **55**, 5622, 1971.
- Seaton, M. J., and D. E. Osterbrock, Relative (O II) intensities in gaseous nebulae, *Astrophys. J.*, **125**, 66, 1957.
- Sharp, W. E.,  $NO_2$  continuum in aurora, *J. Geophys. Res.*, **83**, 4373, 1978.
- Sharp, W. E., M. H. Rees, and A. I. Stewart, Coordinated rocket and satellite measurements of an auroral event, 2, The rocket observations and analysis, *J. Geophys. Res.*, **84**, 1977, 1979.
- Swider, W., and R. S. Narcisi, Ion composition in an IBC class II aurora, 2, Model, *J. Geophys. Res.*, **79**, 2849, 1974.
- Swider, W., and R. S. Narcisi, Auroral E region ion composition and nitric oxide, *Planet. Space Sci.*, **25**, 103, 1977.
- Torr, D. G., and M. R. Torr, Review of rate coefficients of ionic reactions determined from measurements made by the atmosphere explorer satellites, *Rev. Geophys. Space Phys.*, **16**, 327, 1978.
- Torr, D. G., M. R. Torr, J. C. G. Walker, A. O. Nier, L. H. Brace, and H. C. Brinton, Recombination of  $O_2^+$  in the ionosphere, *J. Geophys. Res.*, **81**, 5578, 1976a.
- Torr, D. G., J. C. G. Walker, L. H. Brace, J. H. Hoffman, A. O. Nier, and M. Oppenheimer, Recombination of  $NO^+$  in the ionosphere, *Geophys. Res. Lett.*, **3**, 209, 1976b.
- Vallance-Jones, A., A model for the excitation of electron aurora and some application, *Can. J. Phys.*, **53**, 2267, 1975.
- Walls, F. L., and G. H. Dunn, Measurements of total cross sections for electron recombination with  $NO^+$  and  $O_2^+$  using storage techniques, *J. Geophys. Res.*, **79**, 1911, 1974.
- Wilson, W. E., Rate constant for the reaction  $N + O_2 \rightarrow NO + O$ , *J. Chem. Phys.*, **46**, 2017, 1967.
- Young, R. A., and O. J. Dunn, The excitation and quenching of  $N(^2P)$ , *J. Chem. Phys.*, **63**, 1150, 1975.

(Received October 24, 1978;  
revised February 12, 1979;  
accepted March 5, 1979.)